Journal of ELECTRONIC MATERIALS, Vol. 36, No. 12, 2007
DOI: 10.1007/s11664-007-0275-5

Regular Issue Paper

Effect of Homogenization on the Indentation Creep of Cast Lead-Free Sn-5%Sb Solder Alloy

R. MAHMUDI,[1,3] A. R. GERANMAYEH,[2] M. ALLAMI,[1] and M. BAKHERAD[1]

1.—School of Metallurgical and Materials Engineering, Faculty of Engineering, University of Tehran, Tehran, Iran. 2.—Department of Mechanical Engineering, Islamic Azad University, South Tehran Branch, Tehran, Iran. 3.—e-mail: mahmudi@ut.ac.ir

Creep behavior of cast lead-free Sn-5%Sb solder in unhomogenized and homogenized conditions was investigated by long time Vickers indentation testing under a constant load of 15 N and at temperatures in the range 321–405 K. Based on the steady-state power law creep relationship, the stress exponents were found for both conditions of the material. The creep behavior in the unhomogenized condition can be divided into two stress regimes, with a change from the low-stress regime to the high-stress regime occurring around $11.7 \times 10^{-4} < (H_V/E) < 18 \times 10^{-4}$. The low stress regime activation energy of 54.2 kJ mol^{-1}, which is close to 61.2 kJ mol^{-1} for dislocation pipe diffusion in the Sn, and stress exponents in the range 5.0–3.5 suggest that the operative creep mechanism is dislocation viscous glide. This behavior is in contrast to the high stress regime in which the average values of $n = 11.5$ and $Q = 112.1$ kJ mol^{-1} imply that dislocation creep is the dominant deformation mechanism. Homogenization of the cast material resulted in a rather coarse recrystallized microstructure with stress exponents in the range 12.5–5.7 and activation energy of 64.0 kJ mol^{-1} over the whole ranges of temperature and stress studied, which are indicative of a dislocation creep mechanism.

Key words: Indentation creep, lead-free solder, hardness, Sn-Sb alloy

INTRODUCTION

Although binary Sn-Pb alloys have long been used in the microelectronics packaging industry, concerns about lead toxicity have resulted in serious restrictions on the use of these lead-containing solders.[1] A great deal of attention has been given to research work to explore the possibility of developing suitable substitutes for the Sn-Pb alloys which offer a unique combination of soldering and mechanical properties. Accordingly, many lead-free Sn-based alloy systems with different alloying elements such as Ag, Zn, Cu and Bi have been developed, and their microstructures and mechanical and soldering properties have been investigated.[2–5] Antimony has also been used as the alloying element in the tin-based systems to provide suitable alternatives for Sn-Pb solder alloys. The near-peritectic Sn-5%Sb alloy, with a melting point of 245°C, has been considered as a potential material for this purpose.[6,7] Owing to its relatively low melting point, the usual operating temperature range of 40–100°C corresponds to high homologous temperatures (0.60–0.72) at which creep is the most important deformation mechanism. It has been reported that, in such cases, the material's resistance to cyclic creep deformation, which results from thermal mismatch between electronics packages and substrates and/or power on/off cycles, is of great concern.[8] Therefore, the creep study of tin-antimony alloys has received a great deal of attention.[6,9,10]

In the indentation creep technique, a constant load is applied on the surface of a sample with a suitable indenter for a period of time. Yielding and creep take place, and, therefore, the indenter penetrates the material. The variation of the indentation size, expressed as diagonal length in the Vickers test, is monitored with dwell time. The

(Received January 19, 2007; accepted May 22, 2007; published online September 21, 2007)

study of time-dependent flow or creep of the material is, therefore, made possible by means of simple hardness tests. These indentation tests are simpler than creep tests because they do not require sample machining and can be carried out on small, simple, flat, specimens.[11,12] There have been many attempts to study the creep behavior of solder alloys and other soft materials by the use of indentation or long time hardness tests. These materials include pure lead,[11] pure tin,[13] the eutectic Sn-37.8%Pb alloy,[13–15] Sn-3.5%Ag,[16] Sn-40%Pb-2.5%Sb peritectic,[17] Pb-9%Sn [18] and Pb-(1.25–4.5)%Sb alloys.[19,20] The creep behavior of the lead-free Sn-5%Sb alloy, however, is mostly studied by conventional creep tests,[4,6,10] room-temperature indentation creep tests,[21,22] impression creep, [23] and by the automated ball indentation (ABI) method.[6]

The objective of our work was to study the effect of homogenization on the creep behavior of the cast Sn-5%Sb solder alloy in the temperature range 321–405 K, using different methods of analysis for indentation creep. We also intended to evaluate the creep deformation mechanisms, based on the stress exponents and activation energies obtained for both conditions of the material.

ANALYSIS OF INDENTATION CREEP

It is generally accepted that the mechanical behavior of metallic materials at homologous temperatures higher than 0.5 can be fairly expressed by the power-law creep in a wide range of strain rates. Thus, for steady-state creep, the high temperature creep rate. $\dot{\varepsilon}$ is described by the power law of the type:

$$\dot{\varepsilon} = B\left(\frac{\sigma}{E}\right)^n \exp\left(-\frac{Q}{RT}\right) \tag{1}$$

where σ is the applied stress, E is the elastic modulus, B is a material parameter, n denotes the stress exponent, Q is the activation energy, T is the temperature, and R is the universal gas constant.

Juhasz et al.[15] studied the creep behavior of a superplastic lead-tin alloy, using Vickers tests, and obtained the stress exponent (n) in steady-state creep of the following form:

$$n = \left[\frac{\partial \ln \dot{d}}{\partial \ln(H_V/E)}\right]_d \tag{2}$$

where H_V is the Vickers hardness number, d is the indentation diagonal length, and $\dot{d}$ is the rate of variation in indentation length. This implies that if $\dot{d}$ is plotted against H_V/E on a double logarithmic scale, a straight line would be obtained, the slope of which would be the stress exponent, n.

Sargent and Ashby[24] carried out hot hardness tests on a wide range of materials and proposed a dimensional analysis for indentation creep. According to their model, the displacement rate of an indenter has been derived as:

$$\frac{\mathrm{d}u}{\mathrm{d}t} = \left[\frac{\dot{\varepsilon}_0}{C_2}\left(\sqrt{A}\right)\right]\left[\left(\frac{C_1}{\sigma_0 E}\right)\left(\frac{P}{A}\right)\right]^n \tag{3}$$

where A is the projected area of indentation, C_2 is a constant, $\dot{\varepsilon}_0$ is the rate at a reference stress σ_0, n is the stress exponent, and P is the applied load. For a pyramid indenter the penetration is proportional to $\sqrt{A}$, i.e.:

$$u = C_3\sqrt{A} \tag{4}$$

Differentiating Eq. 4 with respect to time, and substituting into Eq. 3 gives:

$$\frac{\mathrm{d}A}{\mathrm{d}t} = C_4\dot{\varepsilon}_0 A\left(\frac{1}{\sigma_0 E}\frac{P}{A}\right)^n \tag{5}$$

where C_3 and C_4 are constants. When P is held constant, Eq. 5 can be rewritten as:

$$\left(\frac{1}{H_V}\right)\left(\frac{\mathrm{d}H_V}{\mathrm{d}t}\right) = -C_4\dot{\varepsilon}_0\left(\frac{H_V}{\sigma_0 E}\right)^n \tag{6}$$

Sargent and Ashby have also derived the following relationship between indentation hardness and dwell time:

$$H_V(t) = \frac{\sigma_0 E}{(nC_4\dot{\varepsilon}_0 t)^{\frac{1}{n}}} \tag{7}$$

where $H_V(t)$ is the time-dependent hardness. Therefore, from Eq. 7 the slope of a plot of $\ln(H_V/E)$ against $\ln(t)$ at a constant temperature is $-1/n$. The activation energy is calculated from the plot of $\ln(t)$ against $1/T$ at constant H_V/E levels, the slope of which provides Q/R.

EXPERIMENTAL PROCEDURE

Materials and Processing

The material used was a Sn-Sb alloy containing 5 wt.% Sb. It was prepared from high-purity tin (99.99%) and a Sn-20%Sb master alloy melted in an electric furnace under inert argon atmosphere and cast into $120 \times 30 \times 13$ mm^3 slabs. To study the effect of homogenization on the creep behavior of the material, we homogenized some of the slabs for 24 h at 450 K. Both unhomogenized and homogenized cast slabs were cut into $2.5 \times 30 \times 12$ mm^3 slices with a wire cut electrodischarge machine. We studied selected samples by optical microscopy to examine the microstructure evolution of the materials. These specimens were polished with 0.25 μm diamond paste, followed by polishing on a microcloth without any abrasive. Etching was carried out with a 2% nitric acid and 98% alcohol solution at room temperature. The structure of the materials was thus revealed, and the average grain size was measured by the grain count method in which an average grain size may be obtained from measurements of

the number of grains per unit area on a polished surface.

Indentation Creep Tests

Square samples with edges of 20 mm and a thickness of 2.5 mm were cut from both the homogenized and unhomogenized slabs. These samples were polished on a microcloth without abrasive and then tested in a home-made, high-temperature, Vickers hardness tester, where the test temperature and time were the only variables. The testing arrangement for the indentation creep test is shown in Fig. 1. The Vickers indenter was mounted in a holder that was positioned in the center of the vertical loading bar. The specimen was placed in an anvil below the loading bar. The stainless steel container was almost filled with ethylene glycol solution covering the whole specimen and indenter. The bath was then heated by resistive coil heating and stirred by argon gas bubbling through the liquid. The bath temperature was continuously monitored with a thermocouple and maintained to within ±2°C. We made indentation hardness measurements on each sample by placing a dead weight of 15 N on the loading bar for dwell times up to 120 min. After each loading schedule, the sample was unloaded and the indentation diagonal length was measured under a traveling microscope. Each reading was an average of at least three separate measurements taken at random places on the surface of the specimens. All the indentations were at least 5 mm away from the edges and from other indentations. The maximum depth of penetration was about 0.2 mm. By controlling the temperature, we were able to carry out the tests in the temperature range 321–405 K.

RESULTS AND DISCUSSION

The variation of indentation diagonal length (d) versus dwell time, at various temperatures, for both the unhomogenized and homogenized conditions is shown in Fig. 2. As shown in this figure, the curves consist of two stages similar to an ordinary creep curve. The first stage of the curve records an increase in the relevant variable with time, with a decreasing rate, followed by a steady-state region where indentation sizes increase linearly with time. As the hardness test is actually a compression test, fracture of the specimen does not occur, and, hence, it is obviously not possible for one to record a third stage of the curve as opposed to what happens in an ordinary creep test. It can be elucidated from Fig. 2 that the indentation creep behavior of the material under both conditions is affected by temperature. As can be observed, both the level and slope of the indentation curves in the steady-state region increase with increasing test temperature. Owing to the low number of data points for each curve, it is important to check the occurrence of a steady state in the creep curves. We did this by interpolating the data points instead of curve fitting and calculating the rates, using a differentiating computer program. The results plotted as the indentation rate versus time are shown in Fig. 3. It is observed that for most of the test temperatures there exists an apparent steady state.

To obtain more accurate n and Q values, we had to take into account the temperature dependence of

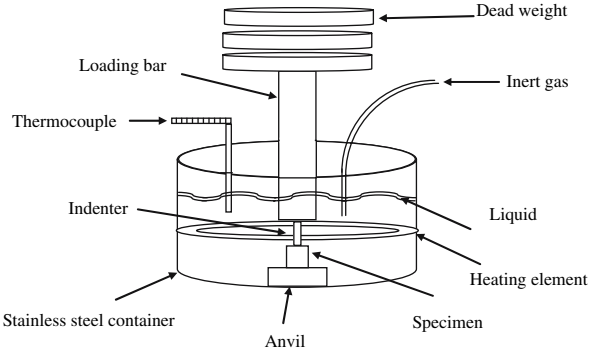

Fig. 1. Schematic illustration of the indentation creep apparatus.

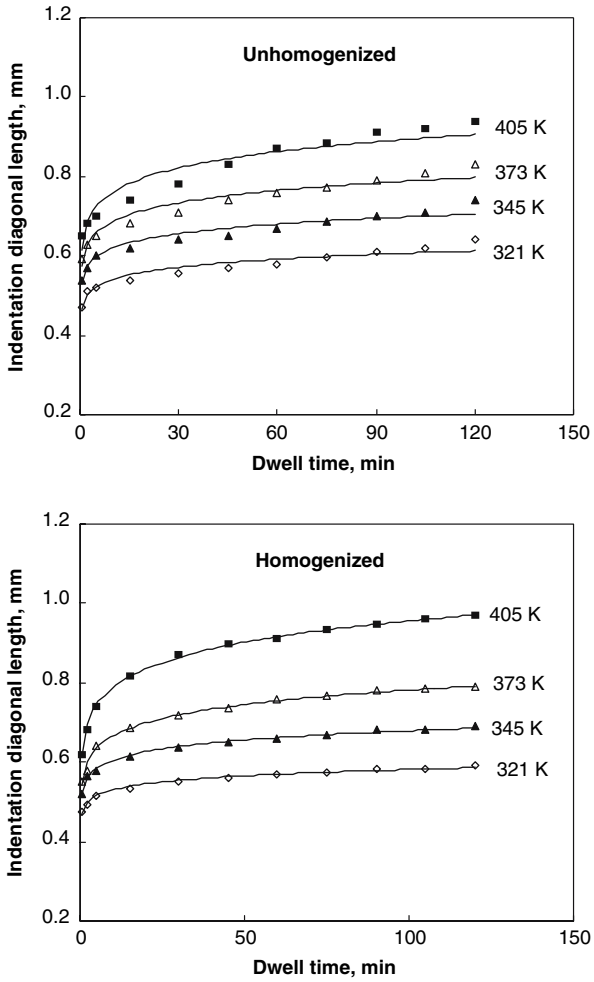

Fig. 2. Indentation creep curves for the unhomogenized and homogenized materials at different temperatures.

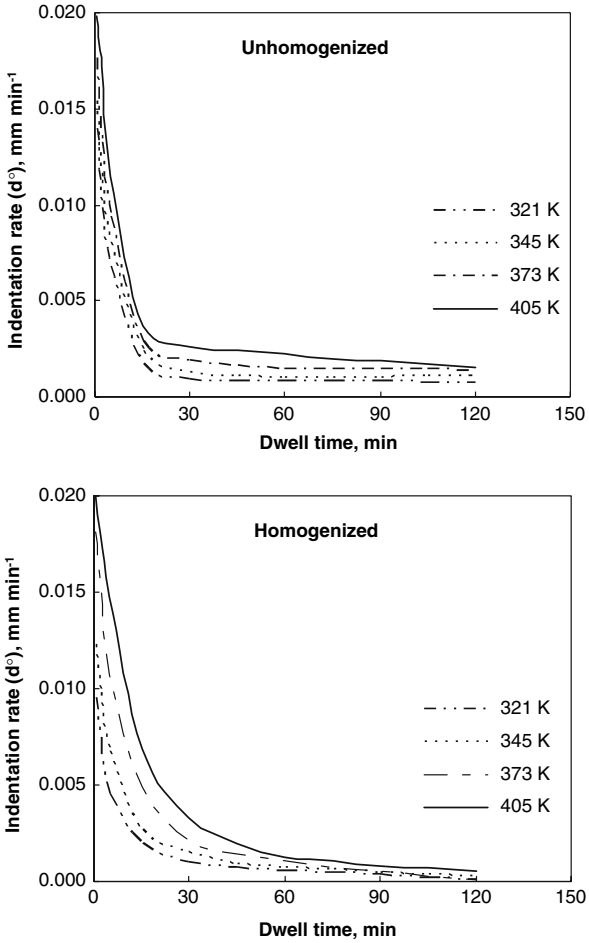

Fig. 3. Variation of indentation rate (d^o) with dwell time for the unhomogenized and homogenized materials at different temperatures.

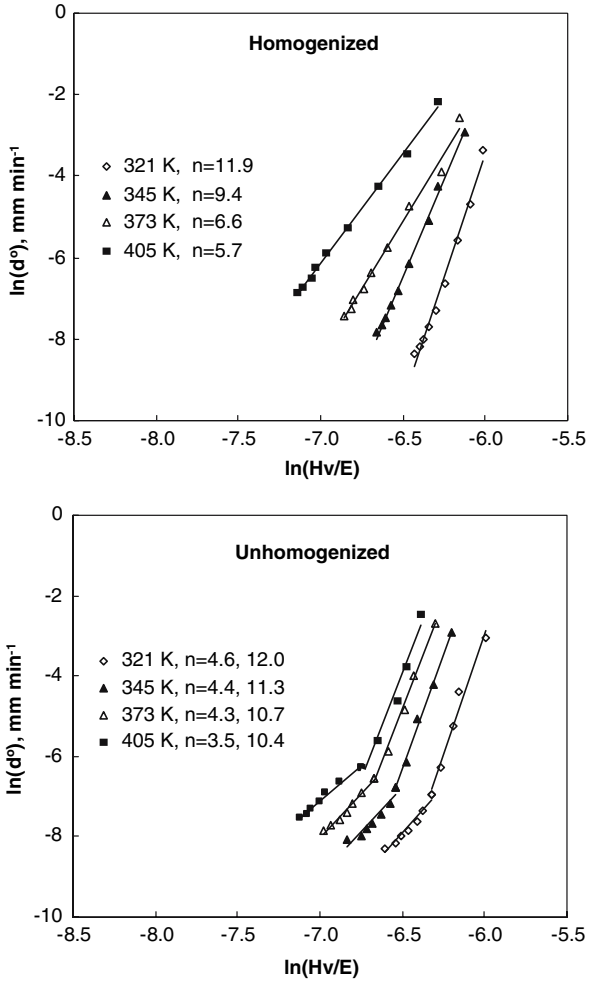

Fig. 4. Plots of ln(d^o) versus ln(Hv/E) at different temperatures to determine the stress exponent.

the elastic modulus. For the dilute Sn-5%Sb alloy, the temperature dependence of elastic modulus of pure Sn can be used. This has been proposed to be obtained from the following equation [25]:

$$E(MPa) = 76,087 - 109T(K) \qquad (8)$$

With the Juhasz et al. method, Eq. 2, the rate of diagonal variation data obtained from the curves in Fig. 3 are plotted against H_V/E on a double logarithmic scale for different test temperatures, as shown in Fig. 4. Different lines with slopes of n result for each condition and temperature. The curves indicate that there are two regions with different slopes in the creep curves for the unhomogenized condition. The transition from the low-stress regime to the high-stress regime occurs in the normalized hardness range $11.7 \times 10^{-4} < (H_V/E) < 18 \times 10^{-4}$ and not at a constant H_V/E level. The low-stress regime shows n values in the range 4.6–3.5, as the temperature increases from 321 K to 405 K. The stress exponents obtained for the high-stress region are in the range 12–10.4. The behavior in the unhomogenized condition is in contrast to that of the homogenized material for which the creep behavior is represented by curves with single slopes, having stress exponents of 11.9–5.7. The stress exponents' ranges calculated in this way are listed in Table I for the two cases.

The alternative method for determining the n value, based on the Sargent–Ashby analysis, considers the variation of H_V/E with dwell time in a log–log scale, as shown in Fig. 5. This figure shows that normalized hardness values decrease with increasing dwell time, due to indentation creep. However, while the hardness of the material in the homogenized condition, measured at different temperatures, can be represented by single linear relationships, the curves for the unhomogenized condition exhibits two sets of parallel lines with different slopes. Similar to the previous method, as the test temperature is increased from 321 K to 405 K, the values of the stress exponents decrease from 12.5 to 6.0 for the homogenized material. For the unhomogenized specimens, however, these variations are from 5.0 to 3.8 for the low-stress regime and from 12.9 to 11.5 for the high-stress regime. These exponents are also given in Table I for comparison. It can be seen that the values of the

Table I. Creep Characteristics of the Material in the Unhomogenized and Homogenized Conditions

Condition	Grain Size (μm)	Stress Regime	Stress Exponent, n		Q (kJ mol^{-1})
			$\ln(d^o)$ versus $\ln(Hv/E)$	$\ln(Hv/E)$ versus $\ln(t)$	
Unhomogenized	35*	Low stress	3.5–4.6	3.8–5.0	54.2
		High stress	10.4–12.0	11.5–12.9	112.1
Homogenized	280	Whole range	5.7–11.9	6.0–12.5	64.0

*Dendrite arm spacing (DAS).

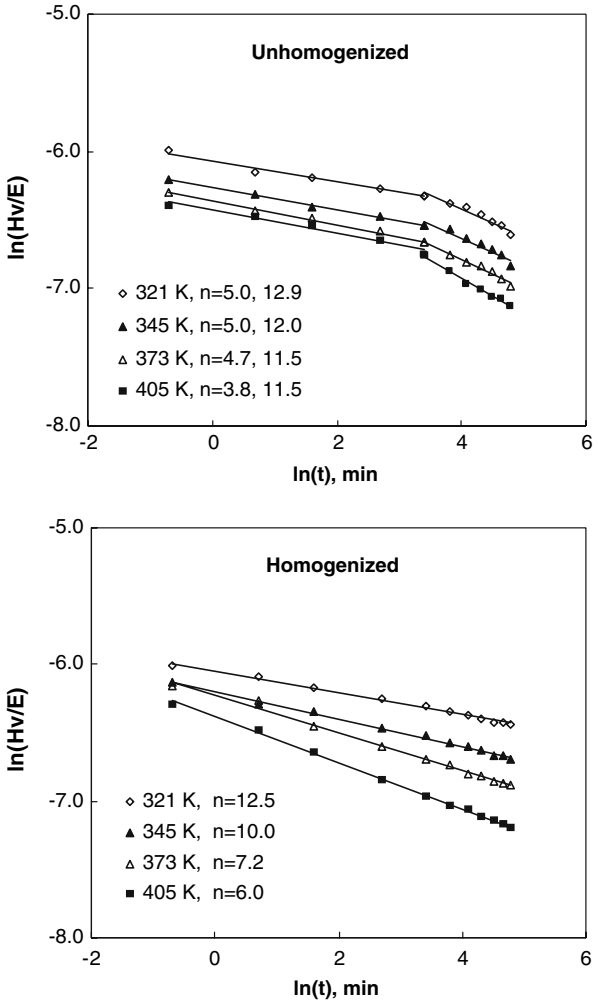

Fig. 5. Normalized hardness–dwell time log–log plots at different temperatures. The slope of these lines will be (–1/n), from which the stress exponent, n, is determined.

stress exponents determined by both methods are in good agreement with each other, indicating the similarity of the derivation methods.

The stress exponents obtained are comparable to those reported in the literature. Stress exponents of 5.4 and 11.4 have been reported for the impression creep of the cast Sn-5%Sb in the low- and high-stress regimes, respectively.[23] Stress exponent values of about 12 and 5 have also been reported for the room-temperature indentation creep of the same alloy in the cast and cold rolled conditions.[21,22] Other similar results obtained in the conventional and automated ball indentation (ABI) creep testing of rolled Sn-5%Sb sheets have yielded n values of 5 in the temperature range of 298–423 K.[6]

The differences observed in the indentation creep behavior of the material in the homogenized and unhomogenized conditions can be attributed to the microstructures of the materials, shown in Fig. 6. It can be observed that the material in the unhomogenized condition has a fine dendritic structure, with a dendrite arm spacing (DAS) of about 35 μm. It seems that the as-cast dendritic structure becomes unstable at long dwell times, resulting in stress exponents which are much less than those obtained in the short dwell time regimes. This is likely because the fast-cooled dendritic microstructure is thermally unstable and has a relatively high potential for coarsening. Such a rapidly cooled microstructure leads to non-equilibrium Sb solute interactions in the β-Sn matrix, producing a viscous drag on gliding dislocations. This is consistent with the operative creep mechanism of dislocation viscous glide in the low-stress regime in the unhomogenized condition. In the high-stress regime, where more dislocation sources become operative, creep is controlled by dislocation interactions, and a transition from dislocation viscous glide to dislocation creep is observed. After homogenization treatment, the dendritic microstructure is completely replaced by a rather coarse recrystallized grain structure with an average grain size of about 280 μm. This results in the reduction of solute supersaturation and a more stable microstructure that does not change significantly, even after long dwell times at temperatures. The consequence of homogenization is thus a more consistent behavior of the material under this condition, with single stress exponents over the whole indentation times at different temperatures.

Concerning the reliability of the creep data, especially for the coarse-grained materials, care must be taken to consider the impact of the comparable sizes of the indentations and the grains. This is likely to cause significant scatter, depending on where the indentation is made, and how many grains contribute to the hardness data obtained.

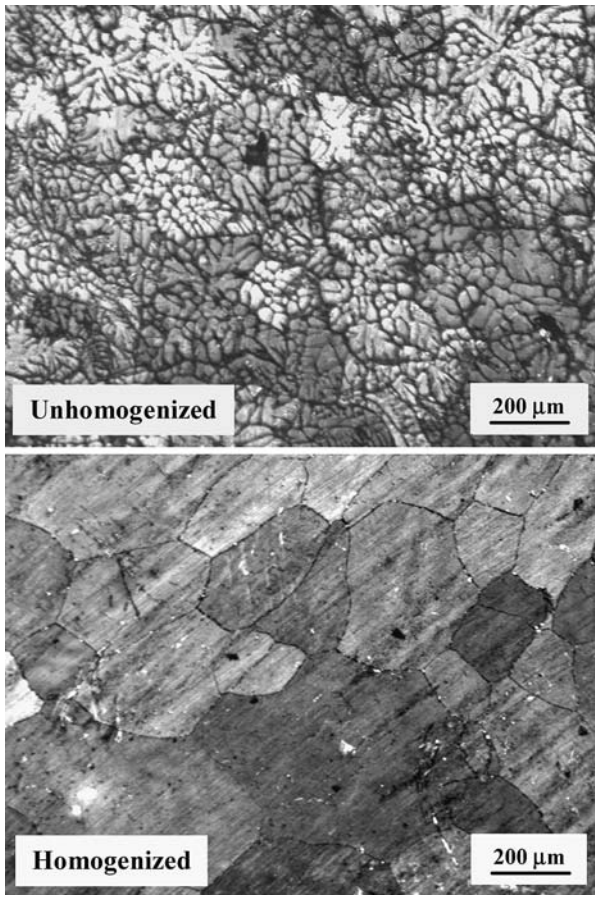

Fig. 6. Optical micrographs of the unhomogenized and homogenized conditions.

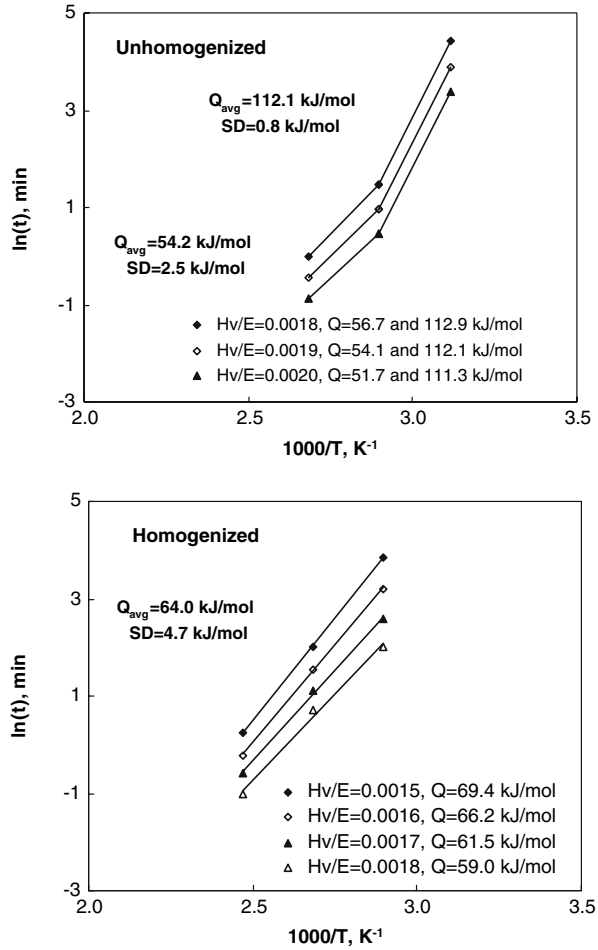

Fig. 7. The variation of dwell time with temperature at different Hv/E levels. The slope of this semi-log plot yields the activation energy for creep.

If only a few grains contribute, the data will become dependent on crystallographic orientation. In the homogenized specimens having a grain size of 0.28 mm, the size of the indentation is of the same order of magnitude as the grain size. Therefore, it was decided to use higher applied loads in which the number of grains participating in the indentation creep process increases and stress exponent values are expected to be more representative. The results, however, indicated that stress exponent values obtained at the higher load of 30 N did not differ significantly from those obtained at 15 N. In the unhomogenized alloy with a relatively fine dendritic structure a large number of grains take part in the indentation process, and, hence, the stress exponent values bear a high level of reliability.

In order to obtain the activation energy values, we plotted $\ln(t)$ against $1/T$ at different constant H_V/E levels, as shown in Fig. 7. Inspection of these curves shows that, for the unhomogenized condition, the average activation energy values of 54.2 kJ mol^{-1} and 112.1 kJ mol^{-1} are obtained for the high temperature (low stress) and low temperature (high stress) regimes, respectively. The very low standard deviations of 0.8 kJ mol^{-1} and 2.5 kJ mol^{-1} found, respectively, for the high and low temperature ranges imply that the activation energies are almost independent of stress and temperature. For the homogenized material, however, the curves exhibit a single linear behavior over the whole range of temperatures and stresses tested, and the activation energy values vary from 59.0 kJ mol^{-1} to 69.4 kJ mol^{-1}, showing a standard deviation of 4.7 kJ mol^{-1}. The activation energy data, together with other characteristics of the materials, are summarized in Table I. The activation energy of 54.2 kJ mol^{-1} is in agreement with the 53.8 kJ mol^{-1} reported for the impression creep of the cast Sn-5%Sb alloy in the temperature range 298–403 K. [23] For material in the homogenized condition, however, the single activation energy of 64.0 kJ mol^{-1} lies between the 53.8 kJ mol^{-1} and 75.8 kJ mol^{-1} found, respectively, for the low stress and high stress impression creep regimes.

It is generally accepted that deformation of polycrystalline materials at temperatures above 0.5 T_m can take place by different deformation mechanisms, associated with different stress exponents and activation energies. According to the theory of dislocation climb-controlled creep, the

stress exponent has the value of 5 and the activation energy has the values of the activation energy of lattice self-diffusion.[26] The theory of dislocation viscous glide, however, leads to a stress exponent of 3 at high temperatures and 5 at low temperatures, the respective activation energies being equal to solute interdiffusion and to dislocation pipe diffusion.[27] The activation energy of 54.2 kJ mol^{-1}, obtained for samples under the unhomogenized condition in the low-stress regime, is close to the activation energy of about 61.2 kJ mol^{-1} reported for the dislocation pipe diffusion (Qp) of Sn.[26] This can be estimated by $Q_p = 0.6\ Q_D$, where Q_D = 102 kJ mol^{-1} is the activation energy of lattice self-diffusion of β-Sn.[28] Stress exponents varied from 5.0 at 321 K to 3.5 at 405 K. These values are in good agreement with the exponent of 5 obtained in conventional creep testing of a Sn-5%Sb alloy.[4] Although the stress exponents of 4.6 and 5.0 found at the lower temperature of 321 K may give rise to the possibility of a climb-controlled mechanism, the activation energy of 54.2 kJ mol^{-1} is much lower than that of lattice self-diffusion (Q_D = 102 kJ mol^{-1}) needed for the climb mechanism. Considering the values obtained for the stress exponents and activation energies, one can infer that dislocation viscous glide could be the dominant creep mechanism for the unhomogenized material in the low-stress regime. This behavior is in contrast to that in the high-stress regime, in which the average values of n = 11.5 and Q = 112.1 kJ mol^{-1} imply that dislocation creep is the dominant deformation mechanism.

Creep behavior of material in the homogenized condition is characterized by an activation energy of 64.0 kJ mol^{-1} and, depending on the temperature, stress exponents of 12.5–5.7. Impression creep testing of the same material has yielded an activation energy of 75.8 kJ mol^{-1} and n values of 11.4 and 5.4 in the high- and low-stress regimes, respectively.[23] Our indentation creep study, however, involved a single creep regime in which stress exponents varied with test temperature. The observed differences could be due to the fact that impression creep is essentially a constant-stress process, while, in the indentation creep tests, the constant load results in decreasing stress, due to the increasing indentation area. It is generally accepted that mechanisms associated with dislocation movement, such as dislocation creep, are attributable to $n > 6$.[29] The high n values of 12.5–6.0, together with an activation energy of 64.0 kJ mol^{-1}, may imply that the operative creep mechanism of material in the homogenized condition is dislocation creep.

CONCLUSIONS

The following conclusions were drawn from indentation creep testing of the homogenized and unhomogenized Sn-5%Sb solder alloy in the temperature range 321–405 K and under a constant load of 15 N.

(1) The indentation creep test was demonstrated to be effective in the evaluation of creep behavior of materials, using small specimens. The data analyses showed that simple theory, based on steady-state power law creep equations, has the capacity to describe the indentation creep data satisfactorily.
(2) The stress exponents calculated from different methods of analysis were in good agreement with each other. The exponents obtained, which decreased with increasing temperature, were found to be 12.5–5.7 for materials in the homogenized condition. For specimens in the unhomogenized condition, however, stress exponents of 5.0–3.5 and 12.9–10.4 were found for the low- and high-stress regimes, respectively. The activation energies showed the same pattern, being 64.0 kJ mol^{-1} for materials in the homogenized condition over the whole range of stress, and 54.2 kJ mol^{-1} and 112.1 kJ mol^{-1} for the unhomogenized material in the low- and high-stress regimes, respectively.
(3) Based on stress exponents and measured activation energies, it can be suggested that, in the homogenized material with a rather coarse grain size, dislocation creep is the dominant creep mechanism. For the unhomogenized condition, dislocation viscous glide and dislocation creep could be the operating creep mechanisms for the low- and high-stress regimes, respectively.

REFERENCES

1. D.G. Kim and S.B. Jung, *J. Alloys Compd.* 386, 151 (2005).
2. R.A. Islam, B.Y. Wu, M.O. Alam, Y.C. Chan, and W. Jillek, *J. Alloys Compd.* 392, 149 (2005).
3. F. Ochoa, X. Deng, and N. Chawala, *J. Electron. Mater.* 33, 1596 (2004).
4. M.D. Mathew, H. Yang, S. Movva, and K.L. Murty, *Metall. Mater. Trans. A* 36A, 99 (2005).
5. N. Wade, K. Wu, J. Kunii, S. Yamada, and K. Miyahara, *J. Electron. Mater.* 30, 1228 (2001).
6. K.L. Murty, F.M. Haggag, and R.K. Mahidhara, *J. Electron. Mater.* 26, 839 (1997).
7. P.T. Vianco and D.R. Frear, *JOM* 45(7), 14 (1993).
8. D. Mitlin, C.H. Raeder, and R.W. Messler, *Metall. Mater. Trans. A* 30A, 115 (1999).
9. H. Mavoori, *JOM* 52(6), 29 (2000).
10. R.J. McCabe and M.E. Fine, *Metall. Mater. Trans. A* 33A, 1531 (2002).
11. A. de La Torre, P. Adeva, and M. Aballe, *J. Mater. Sci.* 26, 4351 (1991).
12. B.N. Lucas and W.C. Oliver, *Metall. Mater. Trans. A* 30A, 601 (1999).
13. M. Fujiwara and M. Otsuka, *Mater. Sci. Eng., A* A319–321, 929 (2001).
14. F. Yang and J.C.M. Li, *Mater. Sci. Eng., A* A201, 40 (1995).
15. A. Juhasz, P. Tasnadi, and I. Kovacs, *J. Mater. Sci. Lett.* 5, 35 (1986).
16. I. Dutta, C. Park, and S. Choi, *Mater. Sci. Eng., A* A379, 401 (2004).
17. R. Mahmudi and A. Rezaee-Bazzaz, *Mater. Lett.* 59, 1705 (2005).
18. T.T. Fang, R.R. Cola, and K.L. Murty, *Metall. Trans. A* 17A, 1447 (1986).
19. R. Roumina, B. Raeisinia, and R. Mahmudi, *Scripta Mater.* 51, 497 (2004).

20. R. Mahmudi, R. Roumina, and B. Raeisinia, *Mater. Sci. Eng., A* A382, 15 (2004).
21. A.R. Geranmayeh and R. Mahmudi, *J. Electron. Mater.* 34, 1002 (2005).
22. A.R. Geranmayeh and R. Mahmudi, *J. Mater. Sci.* 40, 3361 (2005).
23. R. Mahmudi, A.R. Geranmayeh, and A. Rezaee-Bazzaz, *Mater. Sci. Eng., A* A448, 287 (2007).
24. P.M. Sargent and M.F. Ashby, *Mater. Sci. Technol.* 8, 594 (1992).
25. L. Rotherham, A.D.N. Smith, and G.B. Greenough, *J. Inst. Met.* 79, 439 (1951).
26. T.G. Langdon, *Strength of Metals and Alloys.* Proc. 6th Int. Conf., August 1982, ICSMA 6, ed. R.C. Gifkins (Pergamon Press, NY, 1982), p. 1105.
27. T. Reinikainen and J. Kivilahti, *Metall. Mater. Trans. A* 30A, 123 (1999).
28. J.D. Meakin and E. Klokholm, *Trans. TMS-AIME* 218, 463 (1960).
29. B. Walser and O.D. Sherby, *Scripta Matell.* 16, 213 (1982).